GRACE Technical Note 10
(CSR-GR-14-01)

GRAVITY RECOVERY AND CLIMATE EXPERIMENT

Comparison of Degree 60 and Degree 96 Monthly Solutions

(May 5, 2014)

Carly Sakumura
Center for Space Research
The University of Texas at Austin

Prepared by:

Carly Sakumura
UTCSR Graduate Research Assistant

Contact Information:
Center for Space Research
The University of Texas at Austin
3925 W. Braker Lane, Suite 200
Austin, Texas 78759-5321, USA
Email: grace@csr.utexas.edu

Reviewed by:

Srinivas Bettadpur, GRACE Science Operations Manager
UTCSR, Austin

TABLE OF CONTENTS

I INTRODUCTION

I. 1 PURPOSE OF THE DOCUMENT

This document is a comparison analysis of the variations between time-variable gravity fields computed from the NASA/DLR GRACE mission out to degree and order (N_{max}) 60 or 96. The two CSR RL05 fields were analyzed – employing multiple filtering strategies – to see what, if any, differences in solution content and error patterns arose. This analysis was performed in the spectral domain on the spherical harmonic time series as well as in the spatial domain on one-degree gridded time series of equivalent water height (EWH).

I. 2 OVERVIEW OF DATA PROCESSING

This section contains a brief overview of the data processing *differences* between the two solution types, the filtering strategies, and the EWH grid computation. A more complete description of the creation of the Level-2 gravity field data products can be found in the UTCSR Level-2 Processing Standards Document.

The base dataset for both solutions is the regress file, containing the daily mapping matrix and the observational datasets (H, y) from the accelerometer, star camera, inter-satellite range and GPS observations. A monthly 180 x 180 (R, b) matrix is computed from the regress files out to degree and order (d/o) 180 for the given arc of data. The necessary information from this R file is then used to make the solutions out to degree and order 60 or 96 rather than computing each directly from the regress files. The resulting two solutions are essentially the same as if they had been estimated directly from the regress files to the specified maximum d/o and therefore the common first 60 x 60 harmonic coefficients have different numerical values.

In order to account for the noise in the signal, particularly for coefficients of high degree, it is necessary to filter the GRACE solutions. The basic filtering process convolves the GRACE solutions with an isotropic kernel of gradually decreasing power, effectively acting as a spatial low-pass filter on the spherical harmonic coefficients. A common method is Gaussian smoothing which uses an isotropic Gaussian smoothing kernel. The resulting solutions are essentially spatially averaged over the filter-defined smoothing radius. However, there are drawbacks to this process. The filter tends to bias the amplitude towards zero and doesn't account for the variable data density over the surface of the Earth. In addition, the choice of averaging radius is critical as the filter is unable to distinguish between the noise and energy of geophysical signals.

The filtering method proposed in Kusche (2007) is used here. It implements a non-isotropic two-point kernel that uses an a priori synthetic model of the geometry. Unlike the Gaussian filters, the kernel is not axisymmetric and thus takes into account the North-South correlation of the fields. The degree of smoothing can be controlled with the weight of the covariances and the power law within the signal covariance. Thus, this filter removes the striping patterns more effectively than the typical Gaussian filter and is much less likely to bias the data. This is referred to as the DDK filter, and it was chosen to be implemented in the processing of the gravity solutions in this study. There were

three levels of smoothing available, referred to as DDK-1, -2, and -3 where the DDK-1 applies the strongest level of smoothing - approximately corresponding to a Gaussian smoothing radius of 530 km, decreasing through DDK-2 (340 km) to DDK- 3 (240 km).

The EWH grids were computed after the spherical harmonic coefficients were filtered with the specified DDK filter and then converted to one-degree grids of surface mass through the transformation:

$$\Delta\sigma(\theta,\phi) = a_e\rho_w \sum_{l=0}^{\infty}\sum_{m=0}^{l} \bar{P}_{lm}(cos\theta)(\Delta\hat{C}_{lm}cos(m\phi) + \Delta\hat{S}_{lm}sin(m\phi))$$

where $\Delta\sigma$ represents the change in surface density at the specified latitude and longitude dependent upon the Earth's semi-major axis a_e, the density of water ϱ_w, the Legendre polynomials P_{lm}, and the time-varying Level-2 products ΔC_{lm} and ΔS_{lm}.

II SPECTRAL COMPARISON

Format Note: In all figures CSR refers to the Level-2 solution with maximum d/o 60 and C96 refers to that with maximum d/o 96.

II. 1 DEGREE VARIANCE

The degree variance of each time series was computed according to:

$$\sigma_l^2 = \frac{1}{M}\sum_{k=1}^{M}\sum_{m=0}^{l} \delta C_{lm}^2(t_k) + \delta S_{lm}^2(t_k)$$

Multiplying the above equation by the square of the semi-major axis of the Earth allows representation of the degree variance in units of mm geoid. This was performed for eight variations of the Level-2 products – the solutions with N_{max} 60 and 96 unconstrained and with the three levels of filtering, shown in Figure 1.

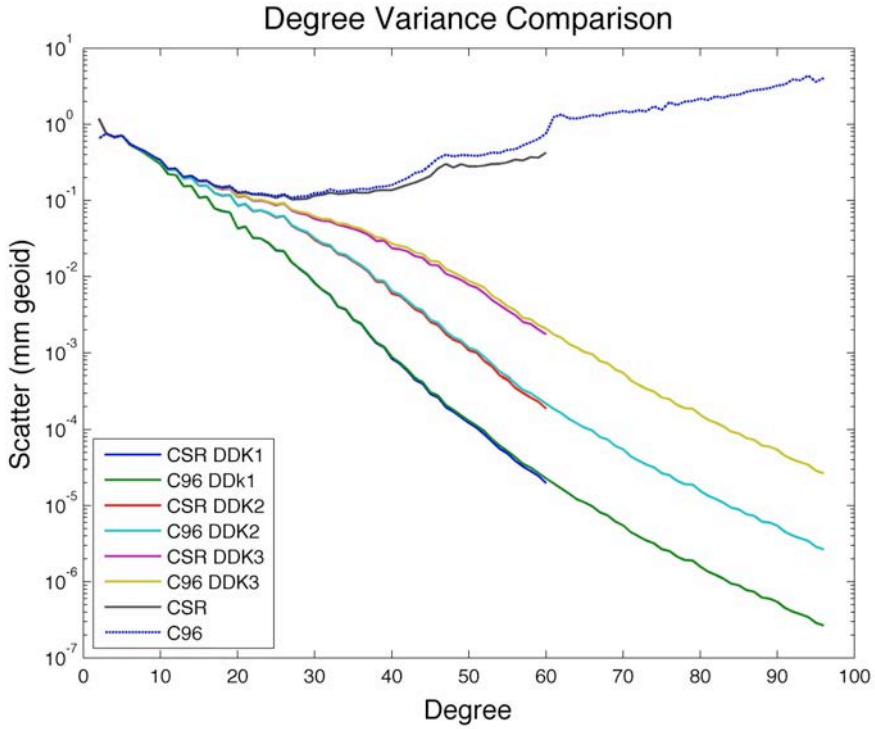

Figure 1: Square Root Degree Variance of d/o 60 and 96 with different smoothing variations

It can be seen that increasing the "amount" of filtering – effectively increasing the smoothing radius – increasingly constrains the harmonics. In each case the solution with N_{max} 96 shows more noise; this is evidenced by the higher scatter present in the degree variance especially at higher degrees. However, this is less pronounced once the coefficients have been filtered, suggesting that the filtering process removes some of the inherent differences between the two solutions.

II. 2 TRIANGLE PLOTS

The other method used to visualize the difference between the two solutions in the spectral domain was through correlation of the spherical harmonic coefficients. This is mapped in triangle plots as shown in the figure below where each colored box represents the correlation coefficient between the N_{max} 60 and C96 time series of a specific harmonic (C_{lm} or S_{lm}) defined as:

$$\rho = \frac{\sum_m \sum_n (A_{mn} - \bar{A})(B_{mn} - \bar{B})}{\sqrt{(\sum_m \sum_n (A_{mn} - \bar{A})^2)(\sum_m \sum_n (B_{mn} - \bar{B})^2)}}$$

This was done for the unconstrained Level-2 products as well as with all three levels of DDK smoothing. It can be seen that, as expected, the correlation of the harmonics is greatly increased post application of the filter. This is particularly evident in the zonal and low-order coefficients. The level of correlation can be seen to increase with increasing filtering and smoothing of the harmonics, therefore the 60 and 96 solutions with the DDK-1 filter are more similar than those where the DDK-3 filter is implemented.

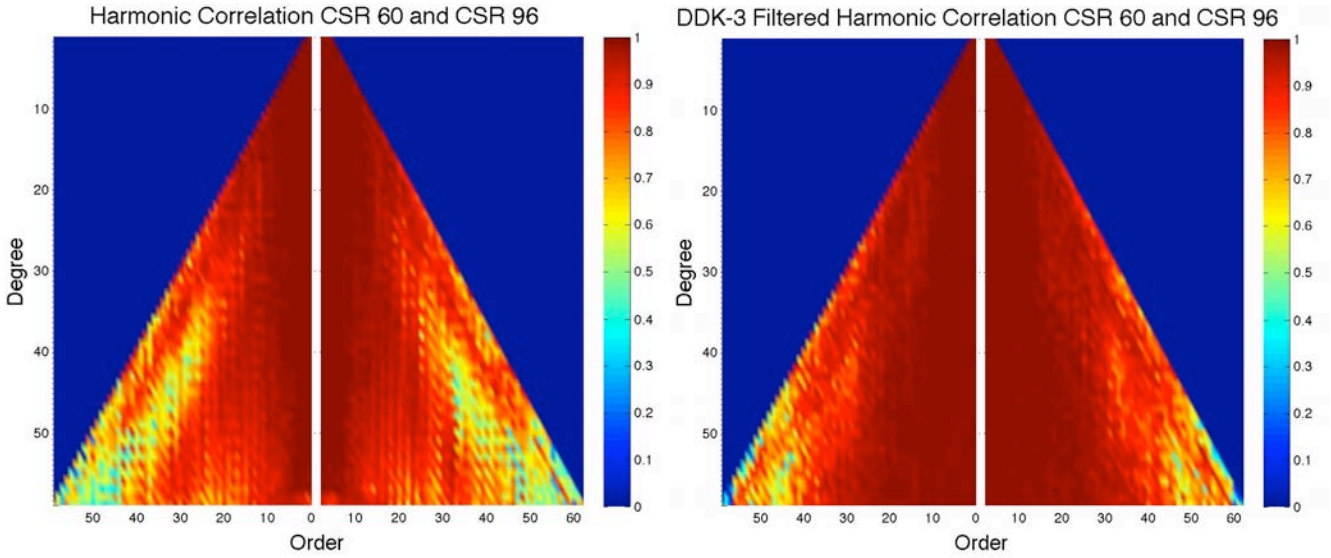

(a) Unconstrained (b) DDK-3

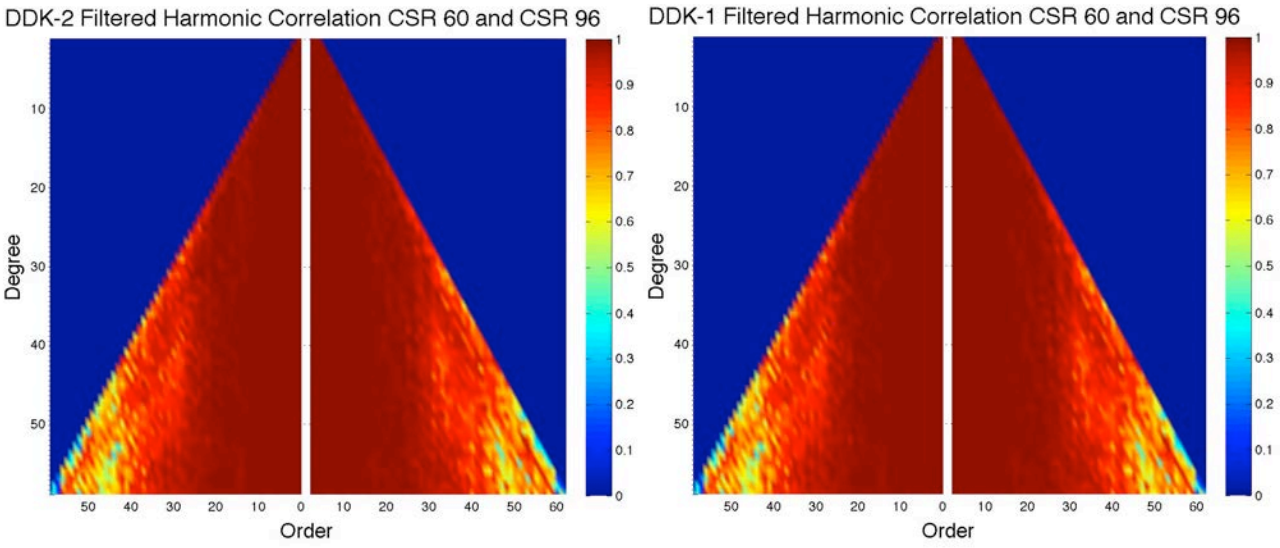

(c) DDK-2 (d) DDK-1

Figure 2: Correlation of the Spherical Harmonic Coefficients with Different Filtering Powers

III SPATIAL COMPARISON

III. 1 EWH GRID COMPARISON

The rest of the analysis will be performed on the EWH gridded datasets to assess the impact of maximum degree solution computation on the physical signal content. In addition, only the DDK-3 and DDK-2 filtered time series will be compared as the unconstrained harmonics are dominated by noise and stripes in the physical domain and it was seen that the DDK-1 filter homogenized the two time series so the differences were nearly negligible. First, this will be analyzed over the entire globe to see if regional or regularly distributed patterns arise. Then, the variations will be compared over global river basins to further assess if the signal content is affected.

III.1.1 Global Variation and Correlation

In order to assess the variations on both short and long time scales several measures were used to compare the two solution types (N_{max} 60 and 96) with the two filtering strengths. The variation was calculated as a direct monthly difference, RMS and mean variation over the time series, and correlation over the time series. The monthly difference maps showed only stripes on the order of noise in the data with no regionally specific patterns. Figure 3 below shows the direct difference between the solutions to N_{max} 60 and 96 for a representative month (April 2006). While the difference has a larger magnitude with the lower level of smoothing in (a), this can be attributed to the higher level of residual noise in the data and not due to signal differences.

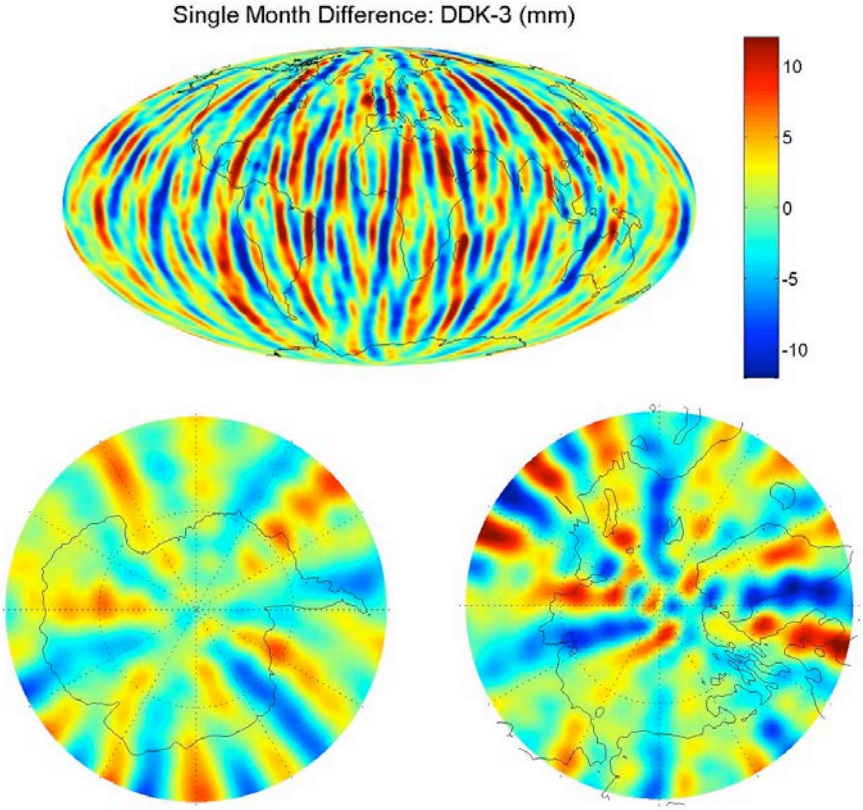

(a) DDK-3

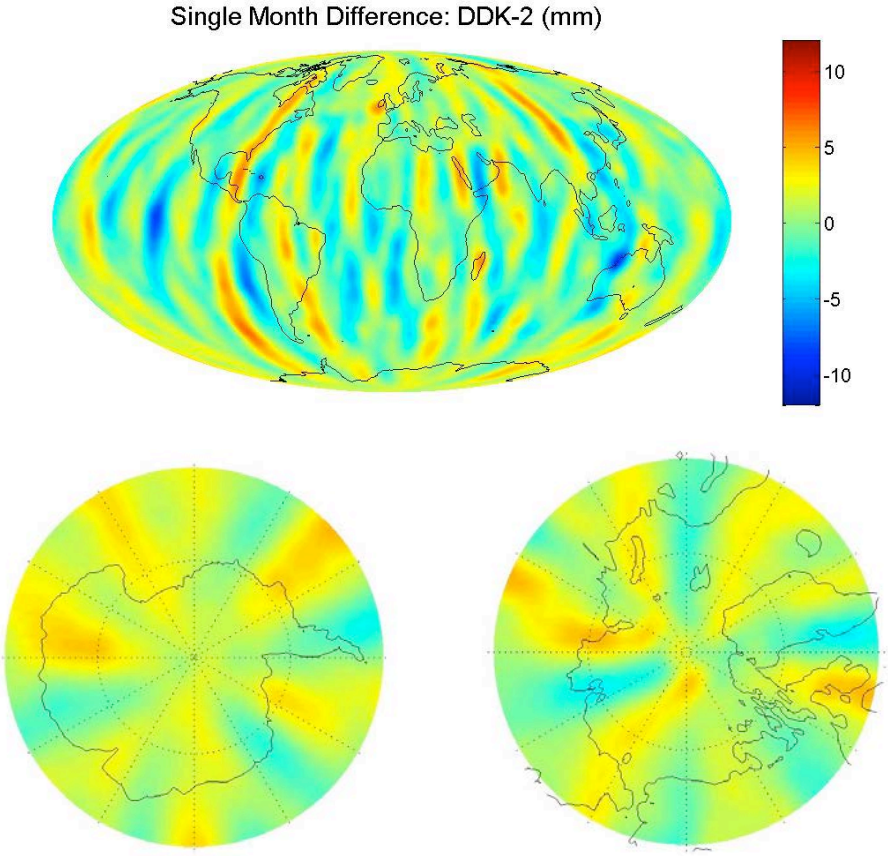

(b) DDK-2

Figure 3: Direct Difference in EWH between N_{max} 60 and 96

Figure 4 shows the RMS difference between the time series of each gridded data point. Again, the difference is seen to be higher in the DDK-3 filtered solutions. However no signal differences arise from the difference and both are on the order of noise in the data.

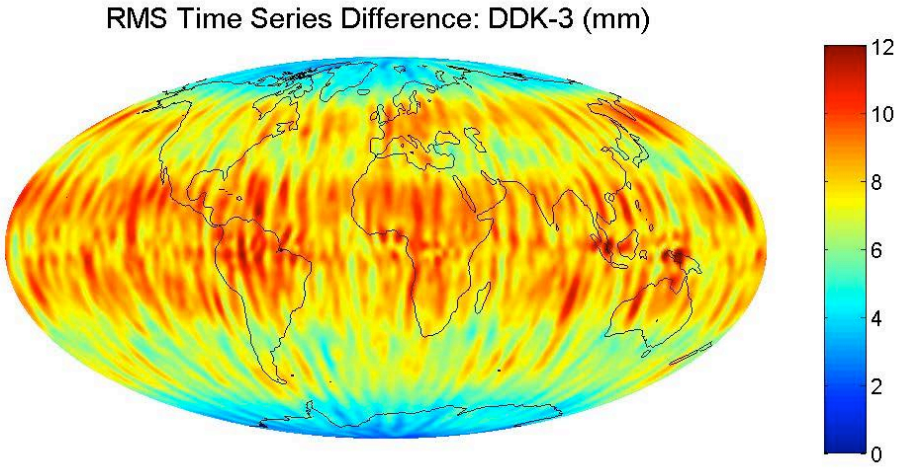

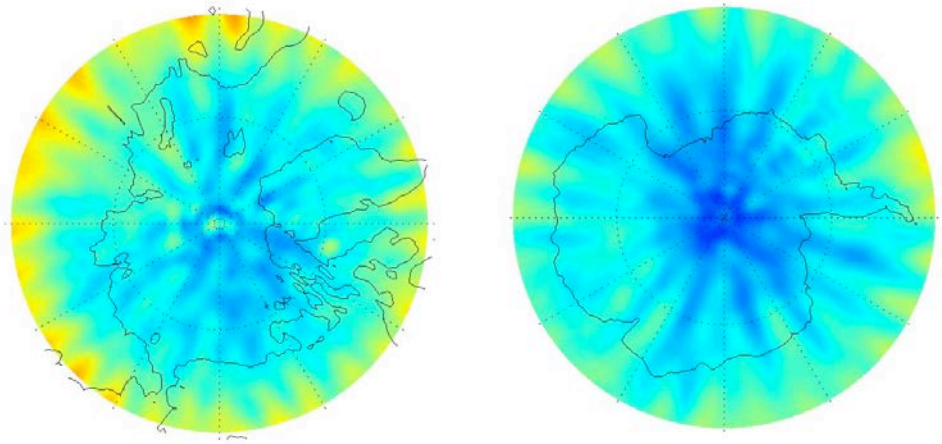

(a) DDK-3

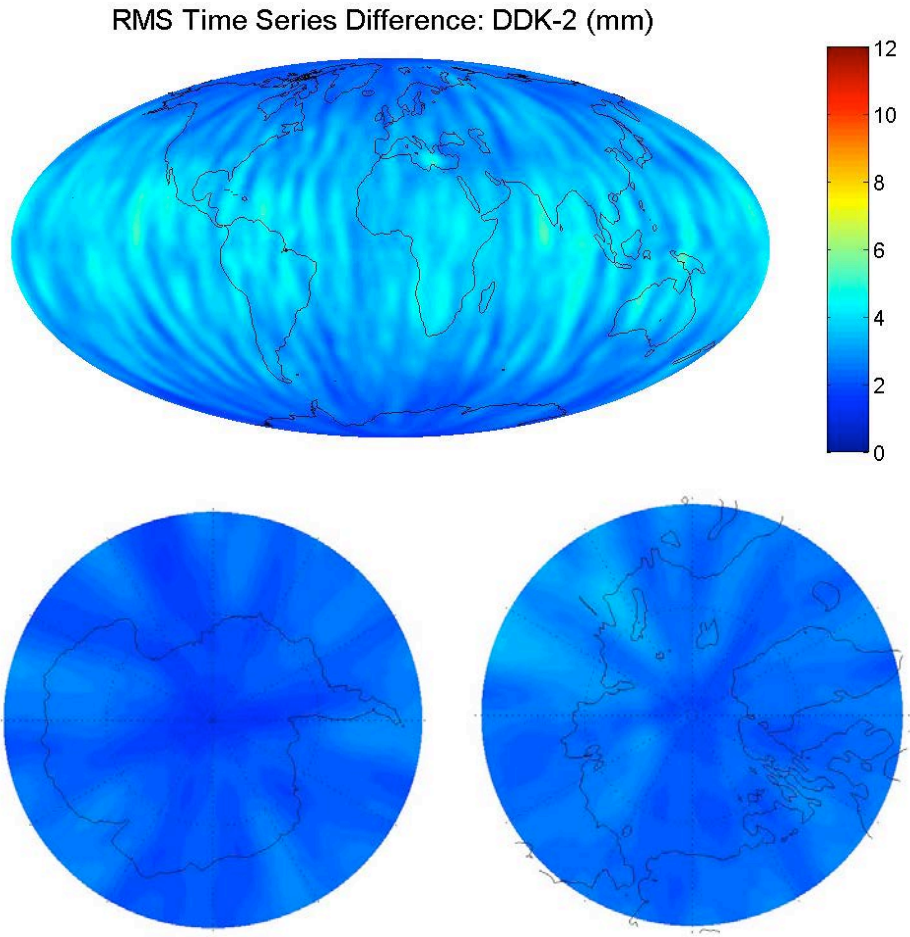

(b) DDK-2

Figure 4: RMS Difference in Time Series between N_{max} 60 and 96

The mean of the time series difference shown in Figure 5 is essentially zero as expected since both series were computed relative to the same epoch. Perhaps more interesting is the correlation between the two solutions, shown in Figure 6. Land processes which

typically are more defined and have larger signal amplitudes than those over oceans thus the land areas appear more highly correlated. This is very clear in Figure 6, even within land areas the more active hydrological regions (i.e. rainforests) show much more correlation than inactive regions such as deserts. In addition, areas of the ocean with signal patterns, such as the gyre off the southern coast of South America, can be identified. Both (a) and (b) show very similar correlation distribution with (b) being more highly correlated again due to the increased smoothing. In addition, the color scale of the figures must be noted – both show very high levels of correlation, very nearly a value of 1 over land.

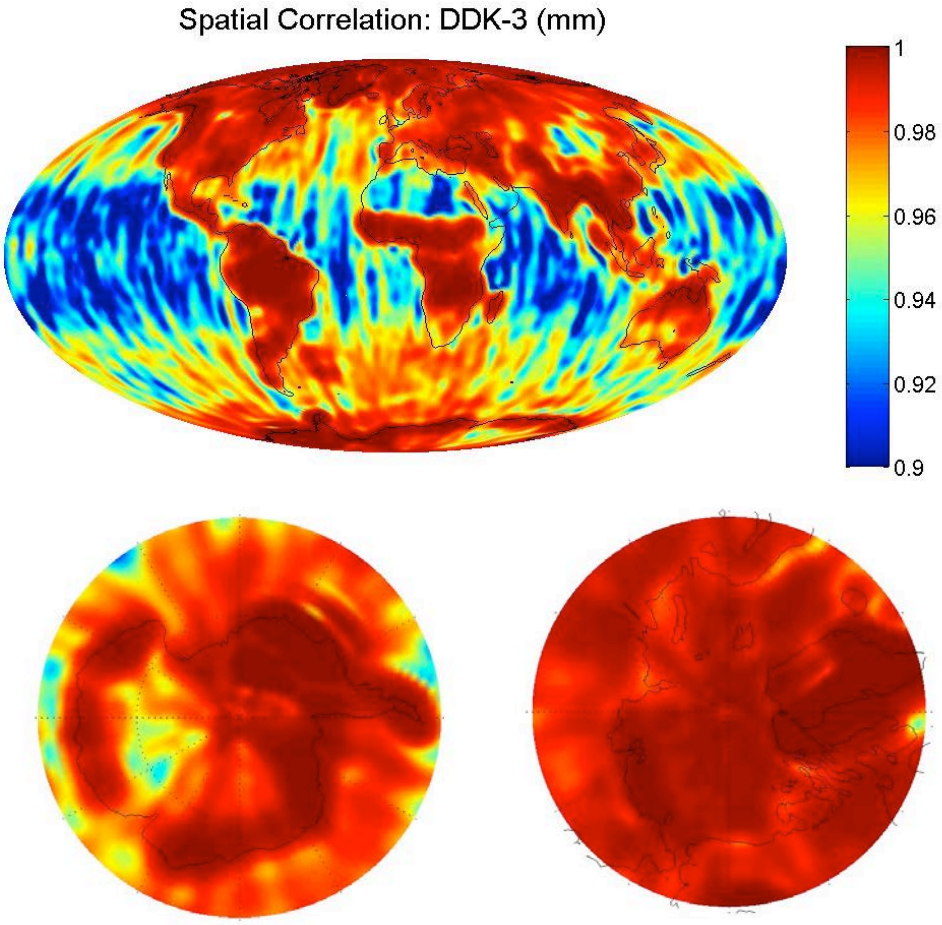

(a) DDK-3

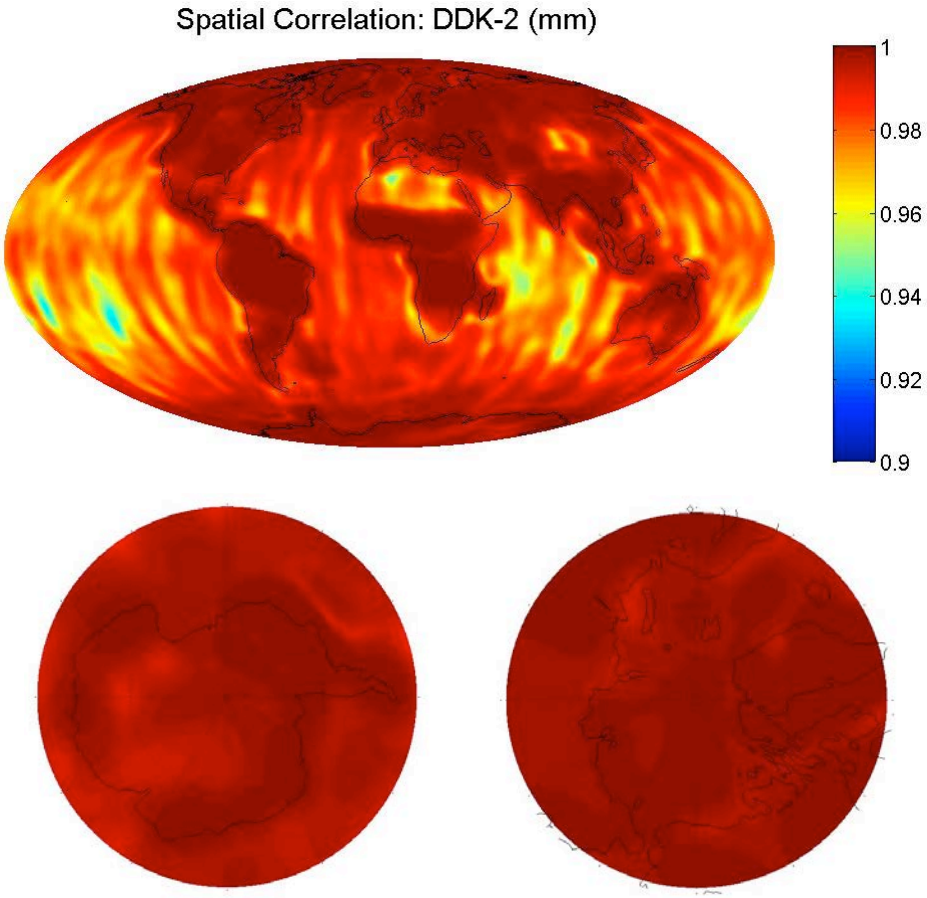

(b) DDK-2

Figure 6: Correlation between N_{max} 60 and 96 Time Series

III.1.2 Basin Scale Variation and Correlation

To further assess whether the maximum degree of 60 or 96 impacts signal content for hydrological applications the solutions are compared over global river basins. The following figures compare the basin mean of the EWH grids. These differences are most generally summarized in Figure 7. Figure 7 shows the RMS of each basin time series (thus a general measure of the variability) in order of decreasing basin size – so basin 1 is the Amazon, then the Nile is 2 and continuing. The difference between CSR and C96 is also plotted in red, and can be seen to be much less than the overall basin variation. In 7(a) a slight trend can be seen in the solution difference with basin size, this will be further explored in the following figures.

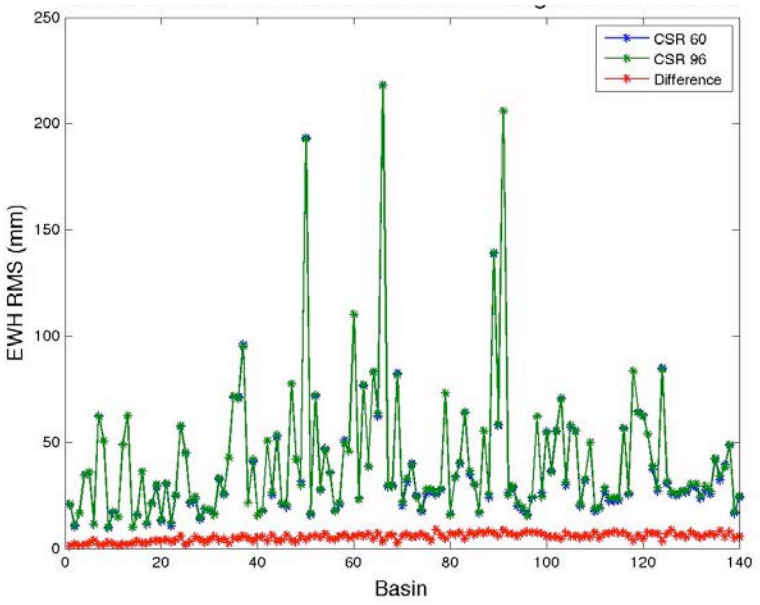

(a) DDK-3

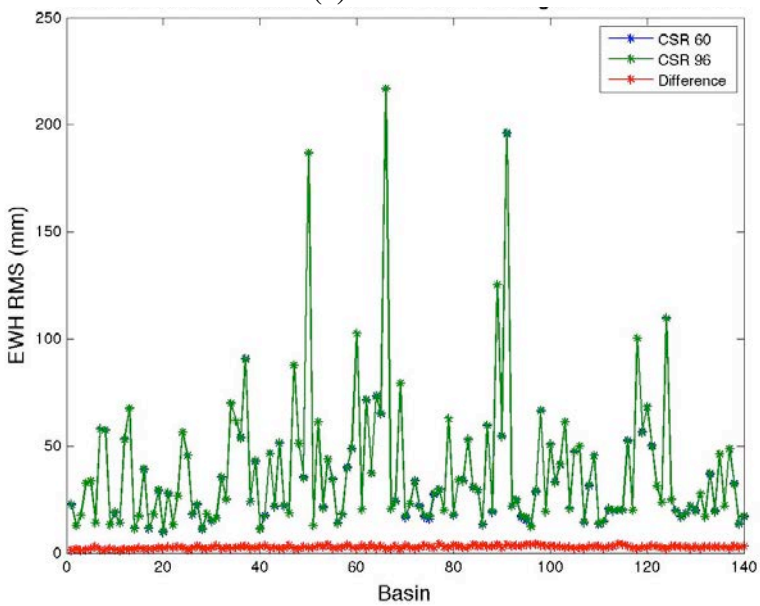

(b) DDK-2

Figure 7: RMS of Basin Mean for N_{max} 60 and 96 and Difference

Further work was done to assess the trend of increasing variation with decreasing basin size identified in Figure 7. To best visualize this, the RMS of the basin time series difference between CSR and C96 was plotted against the size of the basin on a log scale, shown in Figure 8(a). A trend can clearly be seen in the series filtered with DDK-3 and to a lesser extent in those filtered with DDK-2. To compare just the variation scatter, a line was fit to this trend and removed, as shown in 8(b). The larger basins and corresponding larger signals and spatial area to average over will be better and more similarly captured between the two (60 and 96) solutions. The smaller river basins will be more susceptible to the increased noise in the 96 degree solutions, especially when less filtering is applied and therefore show more difference. It must be noted however, that these differences are

all on the level of noise in the GRACE data and therefore assessments on the signal content are very difficult to make on these small (3-4 mm RMS) variations.

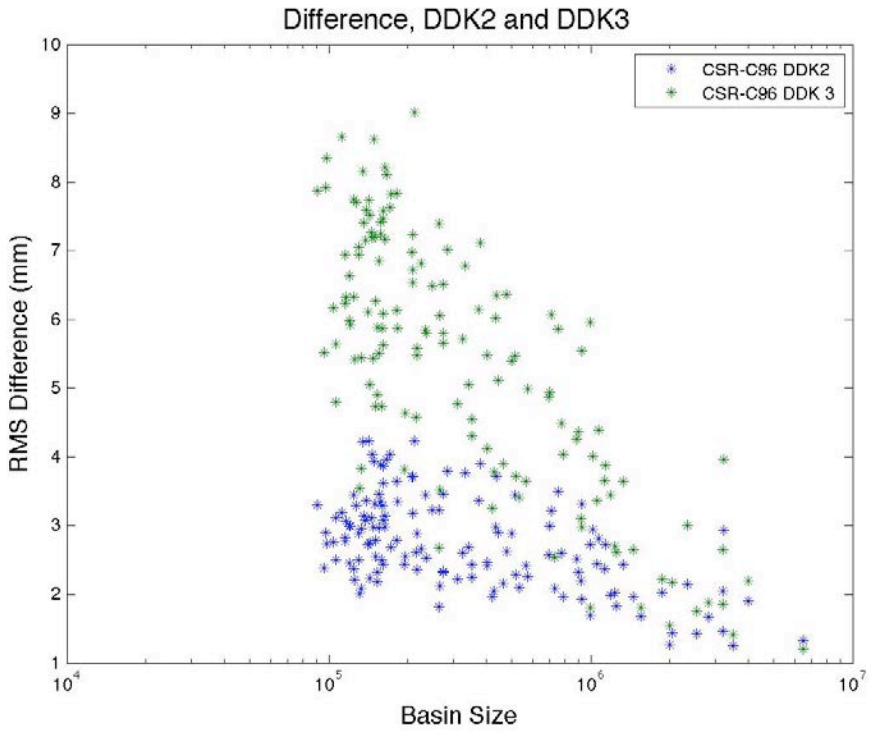

(a)

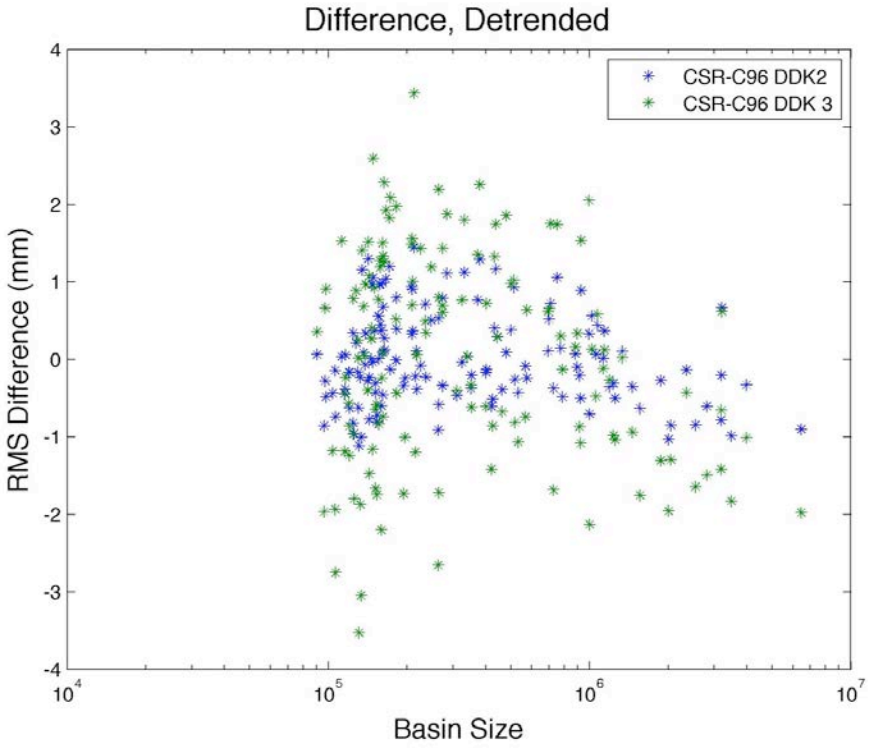

(b)

Figure 8: Basin Variation by Basin Size

To put the variations in perspective, the basin time series for two representative basins, the Amazon and Volga, are shown in Figure 9. Relative to the large scale basin variations, the difference appears quite small and is indeed on the order of noise in the data.

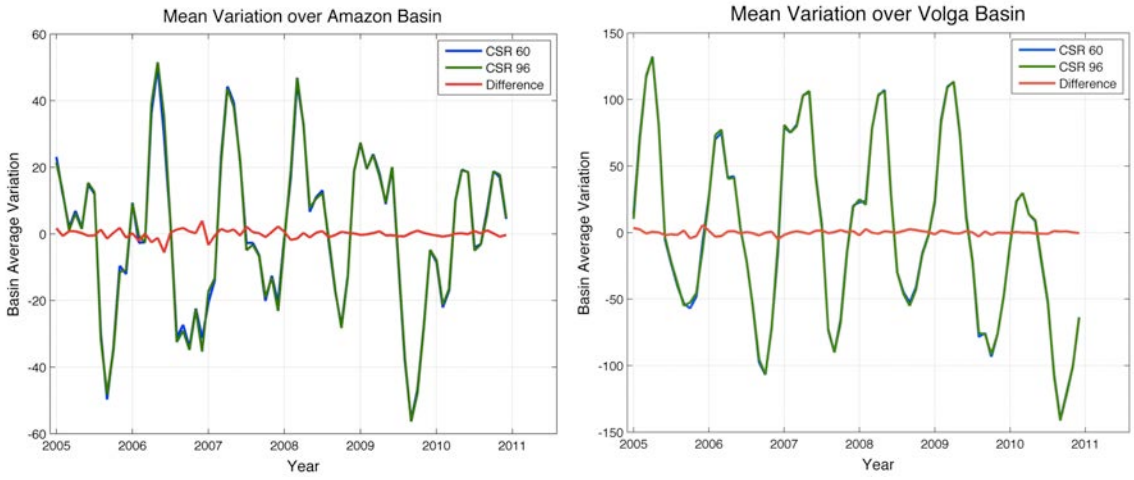

(a) Amazon (b) Volga Basin

Figure 9: Basin Signal Content and Solution Variation

III. 2 COMPARISON ANALYSIS AND VALIDATION

To assess the noise in each solution the solutions/filtering strategies were compared over regions where no or very little variance in EWH is expected. Therefore any EWH variation over time that is found in these regions is assumed to be essentially an estimate of noise in the data. With DDK-2, the noise in the two solutions is essentially the same – only slightly higher for N_{max} 96. With DDK-3 it is evident that the solution to N_{max} 96 has more noise. However, the difference between the two solutions is very small compared to the overall noise level in the data. Thus, the amount of noise in the solution with a higher maximum degree is only very slightly higher when less filtering is applied.

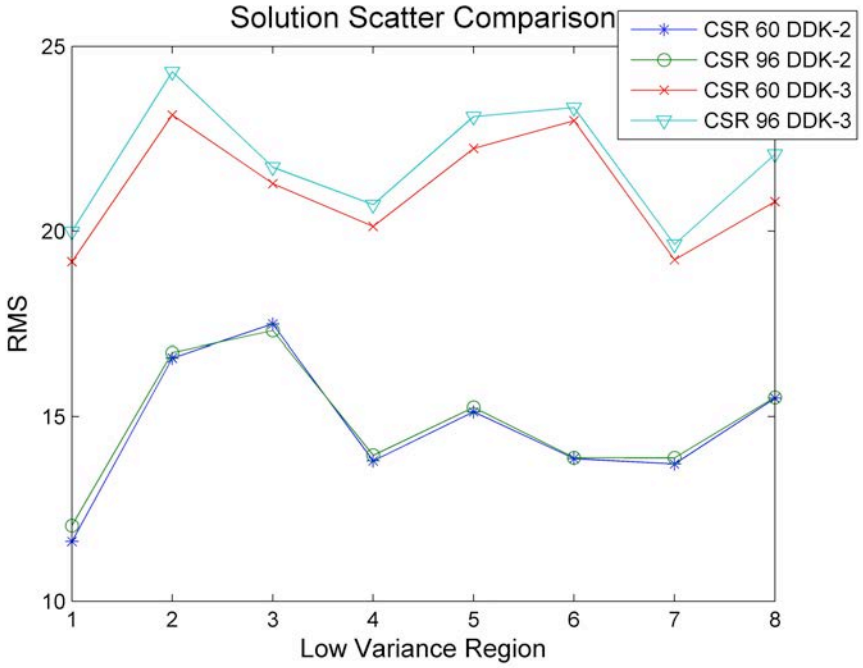

Figure 10: Analysis of the Noise in the Time Series

IV CONCLUSIONS

1. There are no regionally-specific error pattern differences associated with solution computation to d/o 96 or 60
    a. Variations do exist
    b. These are well below the level of noise and appear as stripes in the data
2. Filtering strategies have more of an impact upon solution quality than the maximum degree to which the solution is computed
    a. More variations between the solutions do exist when less filtering/smoothing is enacted upon the fields
    b. This appears to be due to more of the higher level of noise getting through the smaller filter radius as these differences also appear as stripes and are also below the level of noise in the solution
3. Specific applications (e.g. ice sheet melt) particularly in conjunction with different filtering tools than the DDK filter used here could require further investigation